

Damage Features of $\text{Zr}_{41}\text{Ti}_{14}\text{Cu}_{12.5}\text{Ni}_{10}\text{Be}_{22.5}$ Bulk Metallic Glass Impacted by Hypervelocity Projectiles

C. Yang*

South China University of Technology, 510640 Guangzhou, People's Republic of China

and

W. K. Wang,[†] R. P. Liu,[‡] L. Liu,[§] X. Y. Zhang,[¶] and L. X. Li[¶]

Yanshan University, 066004 Qinhuangdao, People's Republic of China

The damage features of $\text{Zr}_{41}\text{Ti}_{14}\text{Cu}_{12.5}\text{Ni}_{10}\text{Be}_{22.5}$ bulk metallic glass under hypervelocity impact were investigated by firing aluminum projectiles with a two-stage light gas gun. Scanning electron microscope results show that radial and symmetric cracks form on the shocked surface of the bulk metallic glass target at the impacted location by a planar aluminum flyer with the velocity of 2.7 km/s. Shear bands/cracks parallel to each other on the cross section close to the shocked surface of the target are observed. The damage features under the spherical aluminum projectiles' impact were also examined. It is shown that besides formation of the similar adiabatic shear bands/cracks, the craters and the lamination cracks are formed, and the depth of the craters increases with increasing projectile velocity.

I. Introduction

MULTICOMPONENT $\text{Zr}_{41}\text{Ti}_{14}\text{Cu}_{12.5}\text{Ni}_{10}\text{Be}_{22.5}$ bulk metallic glass (BMG) with extremely high-glass-forming ability and great engineering application potential,^{1,2} one of the most widely studied BMGs,³ has recently gained considerable attention due to its low density, high strength and fracture toughness, good resistance to corrosion and wear, and unique characteristics of dynamic deformation such as adiabatic shear banding. In recent years, this specific alloy has already reached commercial application potential, such as in the headway in golf clubs.¹ The BMG is also a likely candidate for a space vehicle material. The BMG used for spacecraft might face a danger of collision by space debris and micrometeoroids. To protect space vehicles against the impact of space debris and micrometeoroids, knowledge of dynamic properties of the BMG impacted by hypervelocity projectiles must be obtained. A deal of research on the damage behavior of the BMG under the uniaxial compression,^{4–6} tensile tests,^{7,8} and shocking loading by a powder gun loading system⁹ has been carried out. These studies placed particular emphasis on obtaining the low- and medium-strain-rate response of the BMG. In this paper, we report the damage features on a $\text{Zr}_{41}\text{Ti}_{14}\text{Cu}_{12.5}\text{Ni}_{10}\text{Be}_{22.5}$ BMG caused by accelerated aluminum projectiles with a two-stage light gas gun.

II. Experimental Procedure

The ingots of the alloy with a nominal composition of $\text{Zr}_{41}\text{Ti}_{14}\text{Cu}_{12.5}\text{Ni}_{10}\text{Be}_{22.5}$ were prepared from a mixture of the pure elements in an arc-melting furnace under titanium-gettered argon atmosphere. The purities of Zr, Ti, Cu, Ni, and Be were 99.999, 99.9, 99.5, 99, and 99.5%, respectively. The ingots were crushed into pieces, which were remelted in a quartz tube and then quenched into water to obtain a BMG rod. The structure of the BMG was identified to be in a fully amorphous state by x-ray diffraction. Small cylinders with a length of 10 mm, cut from the alloy rod, were utilized as the target to be collided. The targets were mounted in a sample holder, as shown in Fig. 1. The amorphous cylinder target was superimposed in alignment with the concave curvature of a copper cylinder with a diameter of 40 mm. A polyethylene cylinder was mounted tightly beneath the copper cylinder and an aluminum cylinder tightly beneath the polyethylene cylinder. Also, a steel cylinder was mounted tightly beneath the aluminum cylinder. Finally, the assembly of these cylinders was inserted into a steel tube with a 40-mm inside diameter and 120-mm outer diameter, the end of which was ringent. The other end of the tube was fixed by bolts. The BMG cylinder targets of diameter 22 mm were impacted by spherical aluminum projectiles of 5 mm in diameter with speeds of about 2.6, 3.2, and 3.7 km/s, respectively. Though the speeds are not very high, they can cause a catastrophic failure of protected layers for space vehicles.¹⁰ As compared with the damage behaviors caused by the spherical aluminum projectiles, a planar shock experiment was carried out using the same sample holder except that the BMG target, with a diameter of 18 mm, was covered by a 2-mm-thick copper plate. In the planar shock experiment, the cylinder aluminum flyer was fired with a speed of 2.7 km/s. The cylinder flyer was designed to be 24 mm in diameter and 2 mm in thickness to avoid the influence of the rarefaction from the sample sides.

The axis of the projectiles is coincident with the sample holder. The projectiles were fired by a two-stage light gas gun. The velocity of the projectiles was measured using an electromagnetic induction method. After the impact tests, the specimens for observation were cut from the impacted targets with an electric spark-cutting machine, then grounded and polished mechanically. The morphologies of the craters, the microstructure changes in the region near the crater, and the deformation damage features of cross section, such as adiabatic shear bands and microcracks, were observed by a XL30 S-FEG high-magnification scanning electron microscope (SEM).

Received 16 December 2004; revision received 24 June 2005; accepted for publication 4 September 2005. Copyright © 2005 by the American Institute of Aeronautics and Astronautics, Inc. All rights reserved. Copies of this paper may be made for personal or internal use, on condition that the copier pay the \$10.00 per-copy fee to the Copyright Clearance Center, Inc., 222 Rosewood Drive, Danvers, MA 01923; include the code 0022-4650/06 \$10.00 in correspondence with the CCC.

*Dr., Guangdong Key Laboratory for Advanced Metallic Materials Processing, College of Mechanical Engineering; also Dr., Key Laboratory of Metastable Materials Science and Technology, College of Materials Science and Engineering, Yanshan University, 066004 Qinhuangdao, People's Republic of China.

[†]Professor, Key Laboratory of Metastable Materials Science and Technology, College of Materials Science and Engineering.

[‡]Professor, Key Laboratory of Metastable Materials Science and Technology, College of Materials Science and Engineering; chaoyang666@hotmail.com.

[§]Master, Key Laboratory of Metastable Materials Science and Technology, College of Materials Science and Engineering.

[¶]Dr., Key Laboratory of Metastable Materials Science and Technology, College of Materials Science and Engineering.

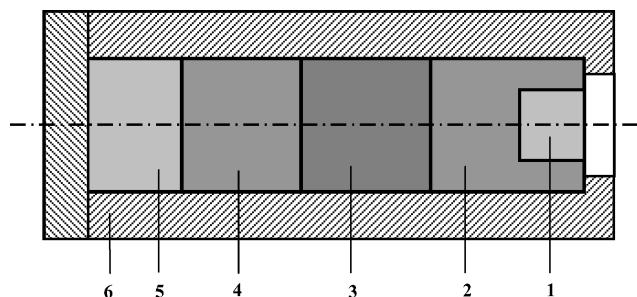


Fig. 1 Schematic of sample holder for high-velocity impact: 1, $\text{Zr}_{41}\text{Ti}_{14}\text{Cu}_{12.5}\text{Ni}_{10}\text{Be}_{22.5}$ BMG target; 2, copper cylinder; 3, polyethylene cylinder; 4, aluminum cylinder; 5, steel cylinder; and 6, steel tube.

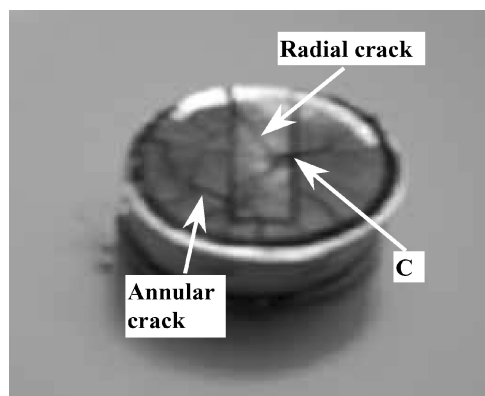


Fig. 2 Optical photograph of shocked surface of $\text{Zr}_{41}\text{Ti}_{14}\text{Cu}_{12.5}\text{Ni}_{10}\text{Be}_{22.5}$ BMG target after planar shock of aluminum flyer at 2.7-km/s speed.

III. Results and Discussion

A. Damage Features Under Planar Aluminum Flyer

The BMG target sample size changes from $\phi 17.5 \times 10$ mm to $\phi 20.5 \times 7.3$ mm under the planar shock loading of the aluminum flyer with a speed of 2.7 km/s. As shown in Fig. 2, the sample upper surface facing the flyer exhibits annular cracks and densely radial cracks initiating from a central point C. The reason for this phenomenon is that the central part of the aluminum flyer could collide first with the central part of the BMG sample because the flyer was hindered by air in the target chamber, making the central part of the flyer blow up forward in the course of flying. Thus compressive shock wave acts initially on the central part of the BMG target, initiating the damage there. The radial cracks propagate from the central point under the action of the strong shock wave. The annular cracks are formed naturally by interaction between the tensile wave reflected from the cylinder copper wall and the compressive shock wave. The recovered aluminum flyer with prominent center along the direction of flying can demonstrate experimentally the discussed phenomenon.

Figure 3 shows the cross-sectional microstructure of the $\text{Zr}_{41}\text{Ti}_{14}\text{Cu}_{12.5}\text{Ni}_{10}\text{Be}_{22.5}$ BMG target after impact by the aluminum flyer with a speed of 2.7 km/s. Several shear bands with a distance of 2 mm are approximately parallel to each other on the upper part of Fig. 3, which cannot be observed clearly due to the limitation of SEM view resolution. The shear bands (as indicated by arrow A), at the angle of 40 deg to the horizontal direction, are formed due to interaction between the shock wave reflected from the cylinder copper wall and the compressive shock wave. This kind of shear band cannot appear in uniaxially compressive and tensile tests. In our case, the sample was impacted, reducing its thickness and expanding its diameter. The shearing along the direction shown by arrow B results in the formation of primarily adiabatic shear band and then induces the secondary shear bands as shown by arrow A. These two shear bands/cracks have already intersected each other. The zigzag-shaped bands (indicated by arrow C) suggest that spalling of the BMG could occur due to brittle damage

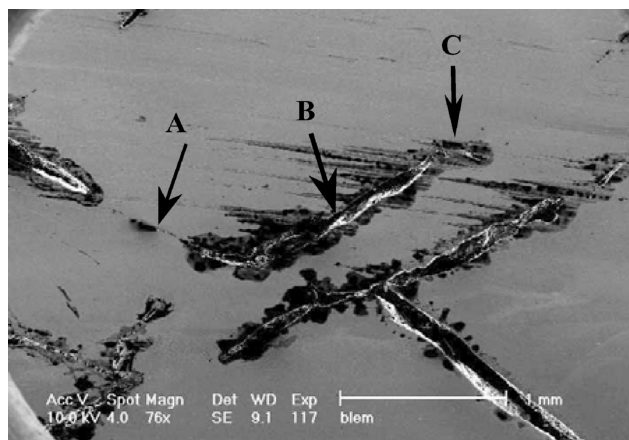


Fig. 3 SEM micrographs showing cross-sectional microstructure of $\text{Zr}_{41}\text{Ti}_{14}\text{Cu}_{12.5}\text{Ni}_{10}\text{Be}_{22.5}$ BMG after planar shock of aluminum flyer at 2.7-km/s speed.

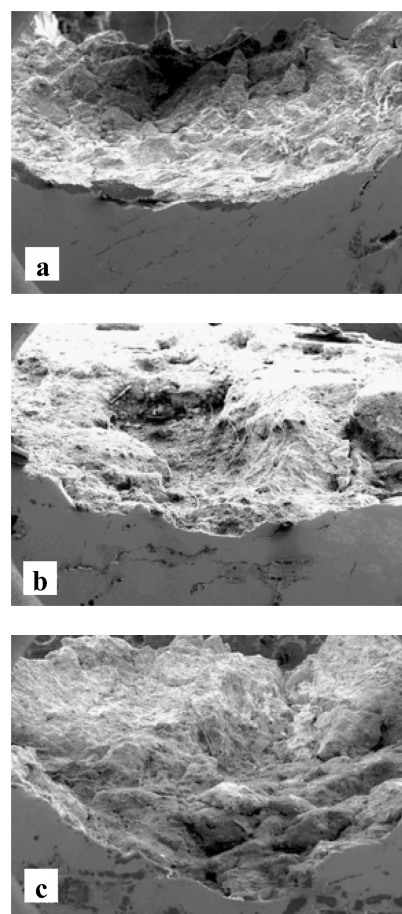


Fig. 4 Cross-sectional morphologies of craters formed on $\text{Zr}_{41}\text{Ti}_{14}\text{Cu}_{12.5}\text{Ni}_{10}\text{Be}_{22.5}$ BMG target with various projectile velocities: a) $v = 2.6$ km/s, b) $v = 3.2$ km/s, and c) $v = 3.7$ km/s.

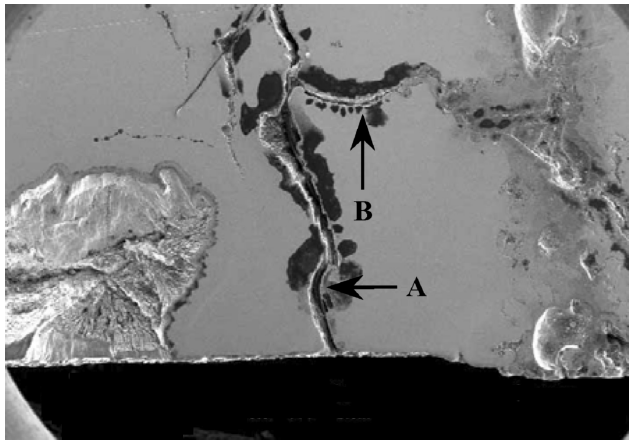
resulting from the shear localization. The shear bands propagate and end at a point where several secondary shear bands form. The secondary shear bands would be propagated with the increase of shock pressure.

B. Damage Features Under Spherical Aluminum Projectiles

Figure 4 shows the cross-sectional morphologies of the craters, which were formed in the $\text{Zr}_{41}\text{Ti}_{14}\text{Cu}_{12.5}\text{Ni}_{10}\text{Be}_{22.5}$ BMG target after the projectiles impact at velocities of 2.6, 3.2, and 3.7 km/s, respectively. The samples, 22 mm in diameter and with a thickness of 10 mm, belong to the medium-thick target type, in which the shock

Table 1 Properties of $\text{Zr}_{41}\text{Ti}_{14}\text{Cu}_{12.5}\text{Ni}_{10}\text{Be}_{22.5}$ BMG compared to metal alloys²

Properties	BMG	Al alloys	Ti alloys	Steels
Density, $\text{g} \cdot \text{cm}^{-3}$	6.1	2.6–2.9	4.3–5.1	7.8
Tensile yield strength, GPa	1.9	0.10–0.63	0.18–1.32	0.50–1.60
Elastic strain limit, %	2	–0.5	–0.5	–0.5
Fracture toughness, $\text{MPa} \cdot \text{m}^{1/2}$	20–140	23–45	55–115	50–154
Specific strength, $\text{GPa} \cdot \text{g}^{-1} \cdot \text{cm}^{-3}$	0.32	<0.24	<0.31	<0.21

**Fig. 5** Typical SEM micrograph showing shear bands/cracks on cross section of BMG target after $\phi 5$ -mm aluminum projectile impact at 3.7-km/s velocity.

wave can interact with the side and back faces, resulting in significant the target damage behavior. It can be seen that the shape of the craters is almost spherical coronary without an obviously outer projecting fringe along the “mouth” of the craters. The crater fringe is extruded from the crater by high pressure and commonly observed on targets impacted by hypervelocity projectiles. The phenomenon without a projecting fringe for the craters may be related to the high strengths and low ductility of the BMG materials. The shape of the craters changes into a spherical shape from the spherical coronary with increasing projectile velocity.

Figure 5 shows a typical SEM micrograph of shear bands/cracks observed on the cross section of the BMG target after the $\phi 5$ -mm aluminum projectile impact with a velocity of $v = 3.7$ km/s. Because the target belongs to a medium-thick type and the projectile is spherical, the shock waves are reflected from the back and side faces of the targets together with the compressive wave, leading to a complicated microdamage. The zigzag-shaped shear band/crack as indicated by the arrow A shows a macrodamage feature caused by the hypervelocity projectile impact. Spallation of the BMG is a more severe damage behavior caused by propagation of the shear bands/cracks. A lamination crack, as indicated by arrow B, with a distance of 2 mm away from back surface is observed. The size of the shear bands/cracks increases with increasing impact velocity.

C. Application Potential of BMG in Aerospace

Table 1 shows that compared to crystalline steel and Ti alloys, the BMG has similar densities but high Young's modulus (96 GPa), Vickers hardness (5.9 GPa), tensile yield strength and elastic strain limit.² These excellent properties may help to make the BMG a possible protective material for spacecraft. Careful observation of the cross section around the crater in Fig. 4a shows that no block body occurs except some adiabatic shear bands/cracks. Li et al.,¹¹ however, found that a block body around the crater was extruded along the adiabatic shear bands after the Ti-6Al-4V alloy target was impacted by the GCr15 steel ball of 4 mm in diameter at a speed of 2.2 km/s. The crater depth for 30CrMnSiA steel target im-

pacted by spherical GCr15 steel projectile with diameter less than 3 mm at 3.2 km/s was 3.0 mm (Ref. 12), whereas the crater depth in Fig. 4b is only 1.9 mm. Therefore, It seems that the BMG is possibly a better protective material for spacecraft, relative to Ti alloys and steel. Nevertheless, because of its low ductility, the BMG exhibits a little plastic deformation before fracture, making it easier to initiate adiabatic shear banding under hypervelocity impact (as seen in Figs. 2–5). This will limit the structural applications in aerospace where reliability is critical. To obtain more tolerance to resistance to shear band and crack propagation, mechanical properties (such as ductility) need to be improved by the preparation of BMG-composites, such as the nanocrystalline-reinforced and the second phase-reinforced BMGs.

IV. Conclusions

The damage features of $\text{Zr}_{41}\text{Ti}_{14}\text{Cu}_{12.5}\text{Ni}_{10}\text{Be}_{22.5}$ BMG caused by hypervelocity impact were investigated by use of a two-stage light gas gun, revealing formation of shear bands/cracks experimentally. Radially symmetric cracks form on the target surface under the planar aluminum flyer impact. Shear bands/cracks that are parallel to each other appear on the cross section close to the shocked surface of the BMG target. The depth of crater in the target increases with increasing spherical projectile velocity in the range of experimental velocity. Also, the shear bands/cracks, together with lamination cracks, were observed on the targets impacted by the hypervelocity projectiles. The BMG could have a potential to be used as a candidate for spacecraft material that resists the impact of small space debris.

Acknowledgments

We thank the National Natural Science Foundation for its support of this research through Grants 50171077 and 50325103.

References

- Inoue, A., “Stabilization of Metallic Supercooled Liquid and Bulk Amorphous Alloys,” *Acta Materialia*, Vol. 48, No. 1, 2000, pp. 279–306.
- Telford, M., “The Case for Bulk Metallic Glass,” *Materials Today*, Vol. 3, No. 3, 2004, pp. 36–43.
- Peker, A., and Johnson, W. L., “A Highly Processable Metallic Glass: $\text{Zr}_{41.2}\text{Ti}_{13.8}\text{Cu}_{12.5}\text{Ni}_{10.0}\text{Be}_{22.5}$,” *Applied Physics Letters*, Vol. 63, No. 17, 1993, pp. 2342–2344.
- Subhash, G., Dowding, R. J., and Kecskes, L. J., “Characterization of Uniaxial Compressive Response of Bulk Amorphous Zr–Ti–Cu–Ni–Be Alloy,” *Materials Science and Engineering A*, Vol. 334, No. 1–2, 2002, pp. 33–40.
- Gilbert, C. J., Ager, J. W., III, Schroeder, V., Ritchie, R. O., Lloyd, J. P., and Graham, J. R., “Light Emission During Fracture of a Zr–Ti–Cu–Ni–Be Bulk Metallic Glass,” *Applied Physics Letters*, Vol. 74, No. 25, 1999, pp. 3809–3811.
- Wright, W. J., Schwarz, R. B., and Nix, W. D., “Localized Heating During Serrated Plastic Flow in Bulk Metallic Glasses,” *Materials Science and Engineering A*, Vol. 319–321, Dec. 2001, pp. 229–232.
- Li, J. X., Shan, G. B., Gao, K. W., Qiao, L. J., and Chu, W. Y., “In Situ SEM Study of Formation and Growth of Shear Bands and Microcracks in Bulk Metallic Glasses,” *Materials Science and Engineering A*, Vol. 354, No. 1–2, 2003, pp. 337–343.
- Flores, K. M., and Dauskardt, R. H., “Crack-Tip Plasticity in Bulk Metallic Glasses,” *Materials Science and Engineering A*, Vol. 319–321, Dec. 2001, pp. 511–515.
- Zhuang, S. M., Lu, J., and Ravichandran, G., “Shock Wave Response of a Zirconium-Based Bulk Metallic Glass and Its Composite,” *Applied Physics Letter*, Vol. 80, No. 24, 2002, pp. 4522–4524.
- Ma, X. H., *Impact Dynamics*, Beijing Inst. of Technology Press, Beijing, 1992.
- Li, H. T., Zhang, Y. M., and Yang, D. Z., “Micro-Damage of Ti–6Al–4V Alloy Under Hypervelocity Projectile Impact,” *Materials Science and Engineering A*, Vol. 292, No. 1, 2000, pp. 130–132.
- Zhou, J. S., Zhen, L., Yang, D. Z., and Li, H. T., “Macro- and Microdamage Behaviors of the 30CrMnSiA Steel Impacted by Hypervelocity Projectiles,” *Materials Science and Engineering A*, Vol. 282, No. 1–2, 2000, pp. 177–182.